

## Sex-specific signatures of intrinsic hippocampal networks and regional integrity underlying cognitive status in multiple sclerosis

Dumitru Ciolac, Gabriel Gonzalez-Escamilla, Angela Radetz, Vinzenz Fleischer, Maren Person, Andreas Johnen, Nils C. Landmeyer, Julia Krämer, Muthuraman Muthuraman, Sven G. Meuth, Sergiu Groppa

### Angaben zur Veröffentlichung / Publication details:

Ciolac, Dumitru, Gabriel Gonzalez-Escamilla, Angela Radetz, Vinzenz Fleischer, Maren Person, Andreas Johnen, Nils C. Landmeyer, et al. 2021. "Sex-specific signatures of intrinsic hippocampal networks and regional integrity underlying cognitive status in multiple sclerosis." *Brain Communications* 3 (3): fcab198.  
<https://doi.org/10.1093/braincomms/fcab198>.

# Sex-specific signatures of intrinsic hippocampal networks and regional integrity underlying cognitive status in multiple sclerosis

 **Dumitru Ciolac,<sup>1,2,3,\*</sup> Gabriel Gonzalez-Escamilla,<sup>1,\*</sup> Angela Radetz,<sup>1</sup> Vinzenz Fleischer,<sup>1</sup> Maren Person,<sup>1</sup> Andreas Johnen,<sup>4</sup> Nils C. Landmeyer,<sup>4</sup> Julia Krämer,<sup>4</sup>  **Muthuraman Muthuraman,<sup>1</sup> Sven G. Meuth<sup>5</sup> and Sergiu Groppa<sup>1</sup>****

\* These authors contributed equally to this work.

The hippocampus is an anatomically compartmentalized structure embedded in highly wired networks that are essential for cognitive functions. The hippocampal vulnerability has been postulated in acute and chronic neuroinflammation in multiple sclerosis, while the patterns of occurring inflammation, neurodegeneration or compensation have not yet been described. Besides focal damage to hippocampal tissue, network disruption is an important contributor to cognitive decline in multiple sclerosis patients. We postulate sex-specific trajectories in hippocampal network reorganization and regional integrity and address their relationship to markers of neuroinflammation, cognitive/memory performance and clinical severity. In a large cohort of multiple sclerosis patients ( $n = 476$ ; 337 females, age  $35 \pm 10$  years, disease duration  $16 \pm 14$  months) and healthy subjects ( $n = 110$ , 54 females; age  $34 \pm 15$  years), we utilized MRI at baseline and at 2-year follow-up to quantify regional hippocampal volumetry and reconstruct single-subject hippocampal networks. Through graph analytical tools we assessed the clustered topology of the hippocampal networks. Mixed-effects analyses served to model sex-based differences in hippocampal network and subfield integrity between multiple sclerosis patients and healthy subjects at both time points and longitudinally. Afterwards, hippocampal network and subfield integrity were related to clinical and radiological variables in dependency of sex attribution. We found a more clustered network architecture in both female and male patients compared to their healthy counterparts. At both time points, female patients displayed a more clustered network topology in comparison to male patients. Over time, multiple sclerosis patients developed an even more clustered network architecture, though with a greater magnitude in females. We detected reduced regional volumes in most of the addressed hippocampal subfields in both female and male patients compared to healthy subjects. Compared to male patients, females displayed lower volumes of para- and subiculum but higher volumes of the molecular layer. Longitudinally, volumetric alterations were more pronounced in female patients, which showed a more extensive regional tissue loss. Despite a comparable cognitive/memory performance between female and male patients over the follow-up period, we identified a strong interrelation between hippocampal network properties and cognitive/memory performance only in female patients. Our findings evidence a more clustered hippocampal network topology in female patients with a more extensive subfield volume loss over time. A stronger relation between cognitive/memory performance and the network topology in female patients suggests greater entrainment of the brain's reserve. These results may serve to adapt sex-targeted neuropsychological interventions.

- 1 Department of Neurology, Focus Program Translational Neuroscience (FTN), Rhine-Main Neuroscience Network (rmn2), University Medical Center of the Johannes Gutenberg University Mainz, Mainz 55131, Germany
- 2 Department of Neurology, Institute of Emergency Medicine, Chisinau 2004, Moldova

Received March 9, 2021. Revised May 27, 2021. Accepted July 15, 2021. Advance Access publication August 23, 2021

© The Author(s) (2021). Published by Oxford University Press on behalf of the Guarantors of Brain.

This is an Open Access article distributed under the terms of the Creative Commons Attribution License (<http://creativecommons.org/licenses/by/4.0/>), which permits unrestricted reuse, distribution, and reproduction in any medium, provided the original work is properly cited.

- 3 Laboratory of Neurobiology and Medical Genetics, Nicolae Testemitanu State University of Medicine and Pharmacy, Chisinau 2004, Moldova
- 4 Department of Neurology with Institute of Translational Neurology, University Hospital of Münster, Münster 48149, Germany
- 5 Department of Neurology, Heinrich Heine University, Düsseldorf 40225, Germany

Correspondence to: Sergiu Groppa, MD, PhD

Department of Neurology, Focus Program Translational Neuroscience (FTN)

Rhine-Main Neuroscience Network (rmn<sup>2</sup>), University Medical Center of the Johannes Gutenberg University

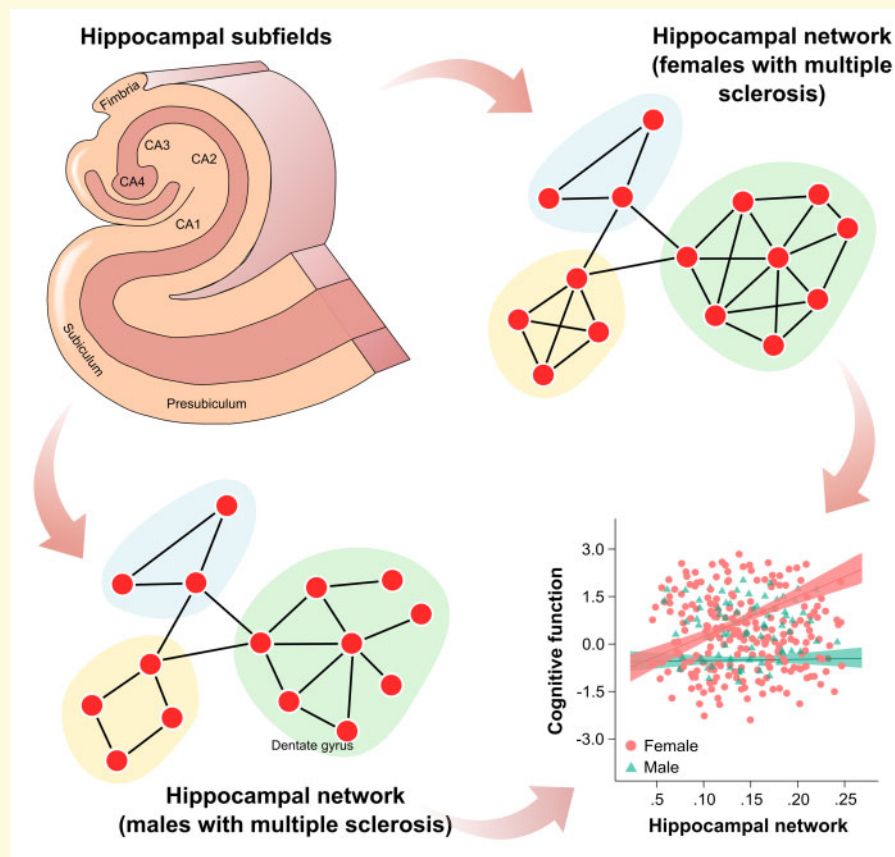
Mainz, Langenbeckstrasse 1, Mainz 55131, Germany .

E-mail: segroppa@uni-mainz.de

**Keywords:** multiple sclerosis; sex-specific signatures; hippocampal networks; hippocampal integrity; cognitive performance

**Abbreviations:** CA = cornu ammonis; EDSS = expanded disability status scale; FA = flip angle; FoV = field of view; FLAIR = fluid-attenuated inversion recovery; GCDG = granule cell layer of dentate gyrus; GM = gray matter; HATA = hippocampus-amygdala transition area; HS = healthy subjects; LMEM = linear mixed effects model; MP-RAGE = magnetization-prepared rapid gradient-echo; MS = multiple sclerosis; MUSIC = Multiple Sclerosis Inventory of Cognition; OASIS-3 = Open Access Series of Imaging Studies; PASAT-3 = Paced Auditory Serial Addition Test 3; RRMS = relapsing-remitting multiple sclerosis; SLIM = Southwest University Longitudinal Imaging Multimodal; TE = echo time; TI = inversion time; TR = repetition time; WM = white matter

## Graphical Abstract



## Introduction

Multiple sclerosis (MS) is an immune-mediated disorder of the central nervous system characterized by focal and diffuse tissue damage, presenting with heterogeneous clinical and imaging phenotypes. It has been proposed that sex might play an important role in this

heterogeneity. While females are at a higher risk of MS, males are more likely to evolve to a progressive disease stage.<sup>1</sup> Findings from neuroimaging studies suggest lower white matter (WM) volumes in female MS patients<sup>2</sup> and more remarkable atrophy of subcortical grey matter (GM) structures in male patients,<sup>3</sup> indicating that sex might shape distinct patterns of brain tissue

vulnerability to neuroinflammatory and neurodegenerative damage in MS. Prior evidence pointed out different trajectories of cognitive impairment in MS patients, males being more prone to cognitive decline with more cognitive domains affected than female patients.<sup>4,5</sup> The mechanisms of sex-specific variability in cognitive performance in MS patients are still elusive. Exploring one of the key component structures in cognitive functioning, the hippocampus might offer valuable insights into the structural correlates of cognitive performance in MS patients.

The hippocampus is a complex functionally and anatomically compartmentalized structure, with a fine-tuned intrinsic network architecture, along with widely distributed connections to other brain networks.<sup>6,7</sup> The integrity of the hippocampal network and subfields organization is essential for maintaining high-order cognitive functions (e.g. learning and long-term memory consolidation).<sup>8</sup> Vulnerability of the hippocampal formation has been recognized from the early stages of MS<sup>9</sup> and is related to cognitive and memory impairment.<sup>10,11</sup> However, measurable patterns of intrinsic hippocampal network and subfield responses to neuroinflammatory and neurodegenerative damage have not been addressed in MS. Moreover, systematic studies on sex-specific effects on hippocampal network and regional organization in MS patients are missing so far. The sex-specific hippocampal network responses can be approached through graph theoretical analysis, which is a unique tool to investigate the alterations of brain networks in MS,<sup>12</sup> providing more sensitive metrics to MS pathology than conventional neuroimaging measures.<sup>13–15</sup>

In light of the above, informing sex-specific signatures of hippocampal networks and regional structural integrity can offer valuable insights into the intrinsic hippocampal organization in MS that may underlie cognitive variability across sexes. Specifically, we test the following hypotheses: (i) morphometric network architecture of the hippocampal formation displays sex-specific differences in MS patients, (ii) regional structural integrity of the hippocampal formation follows the sex-specific network signatures and (iii) both network and regional properties distinctively relate to cognitive performance in female and male MS patients. We address these questions by constructing single-subject morphometric networks and quantifying the volumes of the hippocampal subfields based on high-resolution magnetic resonance images in a large cohort of MS patients. We apply graph theoretical analysis to model the topological organization of reconstructed hippocampal networks at the single-subject level. We relate the network and regional integrity of the hippocampus to a composite cognitive performance score in female and male MS patients. We enhance the presented framework by conducting a longitudinal study over a 2-year time period and including a control cohort of healthy subjects (HS).

## Materials and methods

### Study participants

#### Multiple sclerosis patients

From a large cohort of MS patients, prospectively enrolled at two German Neurology centres (Department of Neurology at the University Medical Center of the Johannes Gutenberg University Mainz and Department of Neurology with Institute of Translational Neurology, University Hospital of Münster), patients with available clinical and MRI data over 2 years were included ( $n=476$ ). The patients were diagnosed with relapsing-remitting MS (RRMS)<sup>16</sup> and had a disease duration of fewer than 5 years (early RRMS). The demographic and clinical characteristics of the patients are summarized in Table 1. To avoid any effects of corticosteroids on MRI-derived hippocampal volumes, patients were steroid- and relapse-free for at least 2 months before scanning.

Clinical (Expanded Disability Status Scale, EDSS), neuropsychological and MRI data were collected at baseline and at 2-year follow-up.

The ethics committee of the State Medical Board of Rhineland-Palatine, of the University of Münster and the Physicians' Chamber of Westphalia-Lippe (Ärztekammer Westfalen-Lippe, 2010-378-b-S, 2017-754-f-S) approved the study and all patients signed the informed consent prior to participation.

#### Neuropsychological assessment

The neuropsychological evaluation was performed by experienced neuropsychologists blinded to patients' clinical and MRI data. This included the Paced Auditory Serial Addition Test 3 (PASAT-3) and the Multiple Sclerosis Inventory of Cognition (MUSIC) test. The PASAT-3 is a cognitive test performed in MS patients to evaluate the attention, working memory and speed of information processing.<sup>17,18</sup> The MUSIC is a cognitive screening test aimed to assess the core cognitive domains impaired in MS—memory, attention, cognitive flexibility and information processing speed.<sup>19</sup> It consists of six subtests: (i) Word List Learning, (ii) Interference Word List Learning, (iii) Category Fluency Switch Condition, (iv) Modified Stroop Task and (v) Word List Recall. Memory is assessed in subtests (i) and (ii) for the immediate recall and in subtest (v) for the delayed recall.

Individual PASAT-3 and MUSIC scores were adjusted for age and education based on the normative data.<sup>19,20</sup> The Z-scores of PASAT-3 and MUSIC tests were averaged to calculate one composite cognitive performance score. Similarly, the Z-scores of memory-related subtests of the MUSIC, that is, Word List Learning, Interference Word List Learning and Word List Recall were averaged to calculate one composite memory performance score. The neuropsychological characteristics of the patients are illustrated in Table 1.

**Table 1** Demographic, clinical, neuropsychological and neuroimaging characteristics of the participants.

	MS (n = 476)			HS (n = 110)			MS vs. HS
	Female	Male	t/Z	Female	Male	t	
Number (%)	n = 337 (70%)	n = 139 (30%)		n = 54 (50%)	n = 56 (50%)		<b>P &lt; 0.001***</b>
Age (years)	35 ± 10	34 ± 9	<b>P = 0.58*</b>	38 ± 12	30 ± 11	<b>P = 0.01*</b>	<b>P = 0.70*</b>
Disease duration (months) EDSS (1–10)	16 ± 11	16 ± 10	<b>P = 0.88*</b>	na	na	na	na
Baseline	1.5 (0–5)	1.5 (0–5)	<b>P = 0.41**</b>	na	na	na	na
Follow-up	1.5 (0–5)	1.0 (0–5)	<b>P = 0.54**</b>				
Composite cognitive performance score (Z-score)							
Baseline	−0.34 ± 1.04	−0.26 ± 0.97	<b>P = 0.53*</b>	na	na	na	na
Follow-up	−0.24 ± 1.07	−0.25 ± 1.04	<b>P = 0.92*</b>				
Composite memory performance (Z-score)							
Baseline	−0.08 ± 0.75	−0.01 ± 0.73	<b>P = 0.47*</b>	na	na	na	na
Follow-up	−0.09 ± 0.88	−0.002 ± 0.84	<b>P = 0.38*</b>				
T2 lesion volume (log <sub>10</sub> mL)							
Baseline	0.38 ± 0.6	0.42 ± 0.6	<b>P = 0.58*</b>	na	na	na	na
Follow-up	0.46 ± 0.6	0.48 ± 0.6	<b>P = 0.76*</b>				
Hippocampal lesion volume (log <sub>10</sub> mL)							
Baseline	0.55 ± 0.32	0.57 ± 0.26	<b>P = 0.78*</b>	na	na	na	na
Follow-up	0.55 ± 0.31	0.60 ± 0.25	<b>P = 0.40*</b>				

EDSS, expanded disability status scale; HS, healthy subjects; MS, multiple sclerosis.

Variables are presented as means ± standard deviation (SD) or median (range).

\*P-values derived from Student's two-tailed t-test (age, disease duration, composite cognitive performance Z-score (average of PASAT and MUSIC Z-scores), composite memory performance Z-score (average of memory-related subtests of the MUSIC test) and T2 and hippocampal lesion volumes).

\*\*P-values derived from Mann–Whitney U-test (EDSS).

\*\*\*P-values derived from Pearson's chi-squared test (sex). Significant P-values are marked in bold.

## Healthy subjects

The demographic and MRI data for the HS group was searched in two open-access longitudinal MRI dataset repositories—the SLIM (Southwest University Longitudinal Imaging Multimodal) Brain Data Repository ([http://fcon\\_1000.projects.nitrc.org/indi/retro/southwest\\_uni\\_qiu\\_index.html](http://fcon_1000.projects.nitrc.org/indi/retro/southwest_uni_qiu_index.html) Accessed 22 May 2019) and the OASIS-3 (Open Access Series of Imaging Studies) MRI database (<https://www.oasis-brains.org> Accessed 22 May 2019). From these two repositories, data available for a 2-year follow-up period were retrieved for 50 HS from SLIM and for 60 HS from OASIS-3 (Table 1). The SLIM database represents a long-term test–retest sample of young healthy adults in southwest China, comprising a large set of longitudinal multimodal imaging<sup>21</sup> from 121 subjects with three MRI sessions. The OASIS-3 represents a data compilation of more than 1000 adult participants and 2000 MRI sessions with multiple structural and functional sequences.<sup>22</sup>

## MRI datasets

### Multiple sclerosis patients

MS patients from first centre underwent MRI scanning at the Neuroimaging Center (NIC), Mainz using a 3T scanner (Magnetom Tim Trio, Siemens, Germany) with a 32-channel head coil. The imaging protocol comprised one sagittal three-dimensional (3D) T<sub>1</sub>-weighted (T1w) magnetization prepared rapid gradient echo (MP-RAGE) and a 3D T<sub>2</sub>-weighted (T2w) fluid attenuated inversion recovery (FLAIR) sequences with the following acquisition

parameters: MP-RAGE—repetition time (TR) = 1900 ms, echo time (TE) = 2.52 ms, inversion time (TI) = 900 ms, flip angle (FA) = 9°, field of view (FoV) = 256 × 256 mm<sup>2</sup>, matrix size = 256 × 256, slice thickness = 1 mm, voxel size = 1 × 1 × 1 mm<sup>3</sup>; T2w-FLAIR—TR = 5000 ms, TE = 388 ms, TI = 1800 ms, FoV = 256 × 256 mm<sup>2</sup>, matrix size = 256 × 256, slice thickness = 1 mm, voxel size = 1 × 1 × 1 mm<sup>3</sup>.

Patients from second centre were imaged on a 3T Siemens Magnetom Prisma<sup>fit</sup> scanner (Siemens, Germany) with a 20-channel head coil and the following acquisition parameters: sagittal 3D T1w MP-RAGE (TR = 2130 ms, TE = 2.2 ms, TI = 900 ms, FA = 8°, FoV = 256 × 256 mm<sup>2</sup>, matrix size = 256 × 256, slice thickness = 1 mm, voxel size = 1 × 1 × 1 mm<sup>3</sup>) and sagittal 3D T2w FLAIR (TR = 5000 ms, TE = 389 ms, TI = 1800 ms, FA = 8°, FoV = 256 × 256 mm<sup>2</sup>, matrix size = 256 × 256, slice thickness = 1 mm, voxel size = 1 × 1 × 1 mm<sup>3</sup>).

### Healthy subjects

Participants from the SLIM database had a high-resolution T1w MP-RAGE sequence (identical with the sequence applied in the first centre) acquired on a 3T MRI scanner (Magnetom Tim Trio, Siemens, Germany). The T1w sequence parameters were: TR = 1900 ms, TE = 2.52 ms, TI = 900 ms, FA = 9°, matrix size 256 × 256, slice thickness = 1 mm, and voxel size = 1 × 1 × 1 mm<sup>3</sup>.

From the OASIS-3 database high-resolution T1w MP-RAGE sequences acquired on a 3T MRI scanner (Magnetom Tim Trio, Siemens, Germany) were extracted. The T1w sequence parameters: TR = 400 ms, TE =



3.16 ms, TI = 1000 ms, FA = 8°, matrix size 256 × 256, slice thickness = 1 mm, and voxel size = 1 × 1 × 1 mm<sup>3</sup>.

## MRI processing

The study pipeline is illustrated in Fig. 1.

### Longitudinal image processing

Cortical surface reconstruction and subcortical volumetric segmentation of every individual T1w image were performed using the FreeSurfer software (version 6.0, <http://surfer.nmr.mgh.harvard.edu/> Accessed 01 December 2017).<sup>23</sup> Then, the longitudinal pipeline, which is based on the creation of an unbiased within-subject template space and image, using robust inverse consistent registration,<sup>24</sup> was applied. All surface models and subcortical segmentations were inspected for accuracy and manually corrected for tissue misclassification or WM errors. To avoid lesion-induced tissue misclassification errors, GM segmentation was performed after filling of T1 hypointense lesions. Cortical and subcortical GM structures were parcellated according to the Desikan–Killiany atlas.<sup>25</sup>

### Hippocampal subfield segmentation

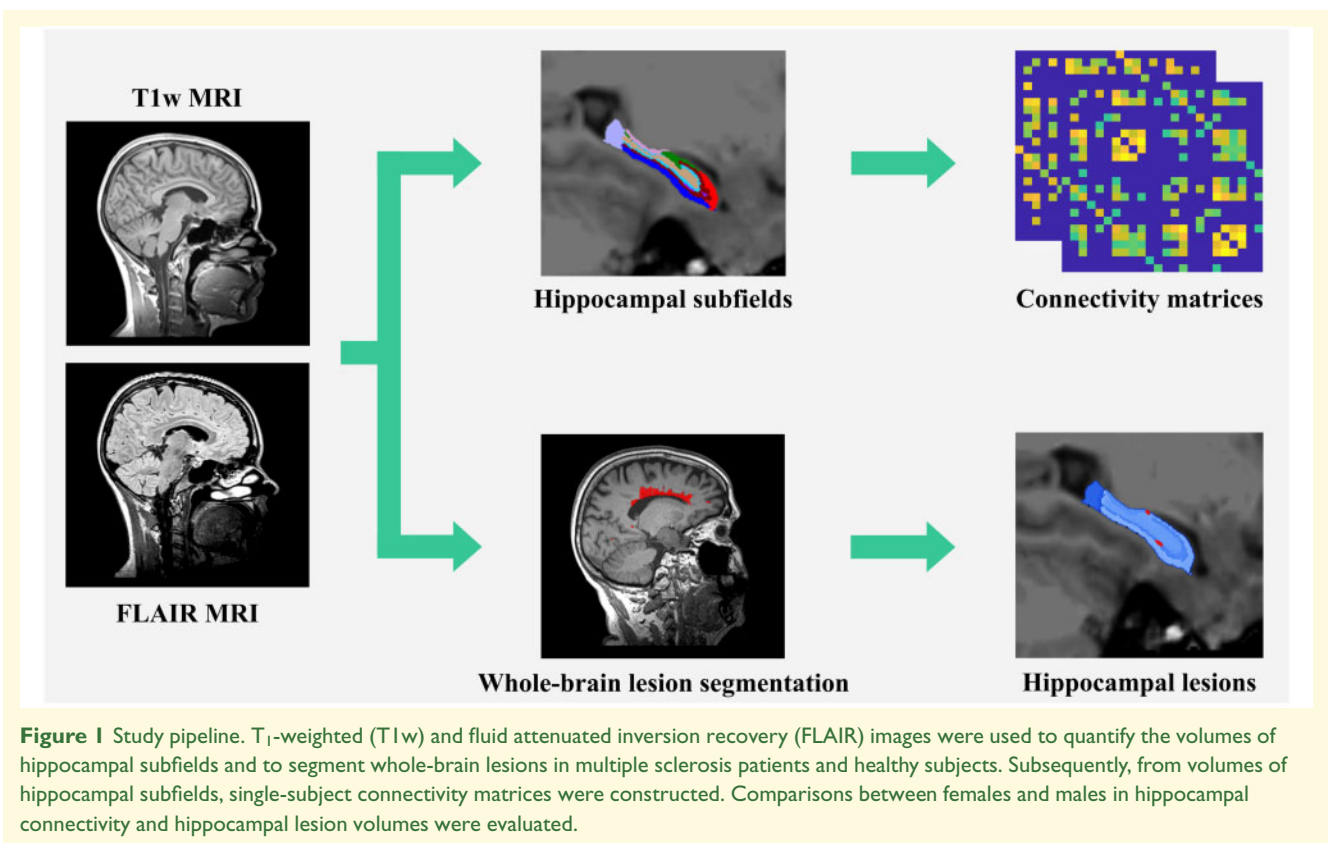
Subject-specific hippocampal subfields were segmented based on the preliminary T1w subcortical segmentation of the whole hippocampus by applying a Bayesian inference approach and a probabilistic atlas of the hippocampal formation.<sup>26</sup> This computational atlas was built upon a

combination of ultra-high resolution (~0.1 mm isotropic) *ex vivo* MRI data from autopsy brains (manual delineation of the hippocampal substructures) and *in vivo* MRI data (manual annotation of the adjacent extrahippocampal structures).<sup>26</sup> The left and right hippocampi were each segmented into 12 subfields per brain hemisphere: parasubiculum, presubiculum, subiculum, cornu ammonis (CA) 1, CA3, CA4, granule cell layer of the dentate gyrus, hippocampus–amygdala transition area, fimbria, molecular layer, hippocampal fissure and hippocampal tail. The automated subfield segmentations were visually inspected and manually corrected where necessary. The FreeSurfer automated hippocampal subfield segmentation shows high accuracy and reliability within and across populations (healthy and diseased),<sup>27</sup> and high stability within and across scanner platforms.<sup>28</sup>

## Network reconstruction and analysis

### Single-subject network reconstruction

Following the hippocampal subfield segmentation into 12 subfields and prior to being entered into the network analysis, hippocampal subfield volumes for all participants (both MS and HS) were adjusted for the variations in total intracranial volume (tVol), age and scanner (Mainz, Münster, SLIM, OASIS-3) in accordance with standard protocols<sup>29,30</sup> using a general linear model:



$$\text{Vol}_{\text{adj}} = \beta_0 + \beta_1 (\text{tVol}) + \beta_2 (\text{Age}) + \beta_3 (\text{Scanner}) + \epsilon$$

where tVol (continuous), age (continuous) and scanner (categorical) are independent variables assumed to explain the dependent variable  $\text{Vol}_{\text{adj}}$ ,  $\beta_0$  is the model intercept and  $\epsilon$  is the residual error. Here, the three  $\beta$ 's are found and represent the degree of variation in  $\text{Vol}_{\text{adj}}$  associated with a variable in the model.

Following volume adjustment, morphometric hippocampal networks for each subject were constructed. Here, nodes represent individual hippocampal subfields and edges represent the volumetric similarity between each pair of subfields, computed as  $\text{Mc}_{(i,j)} = |\text{Vol}_{\text{adj},i} - \text{Vol}_{\text{adj},j}|$ , where Mc is the morphometric connection between the subfields of interest  $i$  and  $j$ .<sup>31</sup> Given 12 hippocampal subfields in each hemisphere, the procedure results in a  $24 \times 24$  fully connected morphometric hippocampal network for each individual.

Identical steps were adopted to reconstruct the whole-brain GM networks (details are provided in the [Supplementary Material](#)).

### Individual network topology computation

We were primarily interested in elucidating the sex-specific signatures of intrinsic hippocampal networks. The topological organization of hippocampal morphometric networks was assessed by using the Brain Connectivity Toolbox (<https://sites.google.com/site/bctnet/> Accessed 10 May 2019)<sup>32</sup> and described in terms of clustering coefficient, modularity, local efficiency and network hub detection. The formulas applied for the calculation of network measures can be found elsewhere.<sup>13,33,34</sup> However, as clustering coefficient, modularity and local efficiency reflect similar features of the local network's organization and showed consistent effects in our analysis, we restricted our results to clustering coefficient.

'Clustering coefficient' is a parameter of local network organization that indicates the number of connections between the neighbouring nodes.<sup>35</sup> Increased clustering coefficient denotes a more strengthened local network connectivity with sparse connections to more distant nodes. 'Network hubs' represent nodes that maintain the efficient organization of the whole network and drive most of the information flows within the network.<sup>36</sup> Definition of a hub was based on the calculation of the betweenness centrality, defined as the number of shortest paths connecting every pair of nodes in the network and crossing through a given node. Hubs were considered those nodes, whose betweenness was two standard deviations above the mean nodal betweenness across the network regions.

### Quantification of hippocampal lesions

For automated calculation of lesion volumes, we employed the lesion segmentation toolbox (LST, <https://www.applied-statistics.de/lst.html> Accessed 10 November 2016),<sup>37</sup> which is part of the statistical parametric

mapping (SPM12) software (<https://www.fil.ion.ucl.ac.uk/spm/> Accessed 25 November 2019). Firstly, whole-brain lesion probability maps were obtained, and afterwards, the hippocampal lesions were quantified by overlapping the hippocampal masks (derived from FreeSurfer) and the lesion probability maps. For this, the 3D FLAIR images were co-registered to the T1w images and bias-corrected. After partial volume estimation, lesion segmentation was performed with 20 different initial threshold values for the lesion growth algorithm. After visual inspection of the resulting lesion probability maps, the optimal threshold of  $\kappa=0.1$  was chosen as the optimal value for all patients. Subsequently, binary lesion maps were grown along the hyperintense voxels in FLAIR images and lesion probability maps were obtained. One advantage of the FreeSurfer subfield segmentation is that its generative nature (Bayesian inference with probabilistic atlas) and unsupervised intensity model (i.e. not segmented based on image intensities), renders this algorithm robustness against changes in MRI contrast, including the presence of lesions.

### Statistical analysis

Statistical analysis was performed using R (version 3.4.2) and RStudio (version 1.1.453), and MATLAB R2017b (Mathworks, Natick, MA, USA). Non-normally distributed data (T2 lesion volume, hippocampal lesion volume) were normalized by logarithmic (base-10) transformation. Demographic, clinical, neuroimaging and neuropsychological characteristics were compared by applying  $t$ -test, Mann-Whitney U-test, Wilcoxon or Pearson's  $\chi^2$ -test, where appropriate.

To determine whether the hippocampal network topology and regional volumetry show sex-specific differences, as well as their association with clinical variables, a set of linear mixed-effects models (LMEMs) as implemented in R (lme4 package), were applied:

- i. Hippocampal network parameters. The dependent term for the model was the network measure (clustering coefficient) with fixed effect terms for the group, sex, time and sex-by-time interaction and with a random intercept term for each participant. As the clustering coefficient is derived from adjusted volumes during the network analysis, the LMEM was run without covariates.
- ii. Hippocampal subfield volumes. The dependent term for each model was the volume of the subfield with fixed effect terms for the group, sex, time and sex-by-time interaction and with a random intercept term for each participant. Separate models were fitted for each hippocampal subfield, which was adjusted for the ICV, age and scanner.
- iii. Relationship between hippocampal network/subfield volume and clinical variables. The relationship between hippocampal network parameters and subfield volumes,

and clinical variables (cognitive/memory performance, EDSS, disease duration) was determined by using LMEMs. Separate models were fitted for female and male MS patients with fixed effect terms for network/subfield measures and with random intercept terms for each participant, and composite cognitive performance as the dependent variable. Similar models were applied for composite memory performance, EDSS and disease duration as dependent variables. The unstandardized regression coefficients ( $B$ ) and standard error of the mean (s.e.m.) are reported.

For all multivariate analyses, post-hoc tests were conducted with Bonferroni correction for multiple comparisons. A  $P$ -value of less than 0.05 was considered statistically significant.

## Data availability

The data of the HS group are available at corresponding MRI repositories—SLIM ([http://fcon\\_1000.projects.nitrc.org/indi/retro/southwestuni\\_qiu\\_index.html](http://fcon_1000.projects.nitrc.org/indi/retro/southwestuni_qiu_index.html)) and OASIS-3 (<https://www.oasisbrains.org>). The de-identified data of MS patients are available from the corresponding author upon a reasonable request.

## Results

### Multiple sclerosis patients remain clinically and cognitively preserved, while accumulating hippocampal lesions

Table 1 contains the demographic, clinical and MR imaging characteristics of MS and HS groups stratified into sex subgroups. No age differences were found between the MS and HS cohorts ( $35 \pm 10$  vs.  $34 \pm 15$  years,  $t = 0.48$ ,  $P = 0.62$ ), between the MS and HS females ( $35 \pm 10$  vs.  $38 \pm 12$ ,  $t = -1.39$ ,  $P = 0.16$ ), nor between the MS and HS males ( $34 \pm 9$  vs.  $30 \pm 11$ ,  $t = 1.64$ ,  $P = 0.09$ ). Only, included HS males were younger than HS females ( $t = 2.63$ ,  $P = 0.01$ ). There were more MS females than HS females ( $\chi^2 = 18.8$ ,  $P < 0.001$ ), while sex distribution was similar between the two centres of the MS cohort (Mainz female/male 158/61 vs. Münster 179/78;  $\chi^2 = 0.62$ ,  $P = 0.42$ ), as well as between the two HS datasets (SLIM female/male 25/24 vs. OASIS-3 29/32;  $\chi^2 = 0.20$ ,  $P = 0.65$ ).

Within MS, there were no significant differences in baseline age, disease duration, EDSS, composite cognitive and memory performance, whole-brain T2 and hippocampal lesion volumes (all  $P > 0.05$ ) between female and male patients (Table 1). Over the 2-year follow-up, patients' disability (as measured by EDSS), composite cognitive and memory performance showed no differences compared to baseline (all  $P > 0.05$ ), while whole-brain T2

and hippocampal lesion volumes increased (both  $P < 0.001$ ).

### Multiple sclerosis females and males display a more clustered hippocampal network organization and lower subfield integrity

The main and interaction effects from the LMEM analysis for hippocampal network topology and subfield volumes are reported in Tables 2 and 3, respectively.

At baseline, female MS patients displayed a higher clustering coefficient compared to their healthy counterparts ( $P = 0.004$ ) (Fig. 2). Similarly, male MS patients presented a higher clustering coefficient ( $P = 0.007$ ) compared to HS males (Fig. 2).

Straightforwardly, at baseline, the differences in hippocampal networks were concurrent with the differences in hippocampal regional integrity. Compared to HS females, female MS patients had lower volumes across almost all hippocampal subfields—parasubiculum, presubiculum, CA1, CA3, CA4, granule cell layer of the dentate gyrus, hippocampus-amygdala transition area, fimbria, molecular layer and hippocampal tail (all  $P < 0.001$ ), except for subiculum, hippocampal fissure and whole hippocampal volume (all  $P > 0.05$ ) (Fig. 3).

Male MS patients showed lower volumes across many subfields—CA1, CA3, CA4, granule cell layer of the dentate gyrus, hippocampus-amygdala transition area, fimbria, molecular layer and hippocampal tail (all  $P < 0.001$ ), except parasubiculum, presubiculum, subiculum and whole hippocampus (all  $P > 0.05$ ) compared to HS males (Fig. 3).

### Multiple sclerosis females compared to males display a more clustered hippocampal network organization and compromised regional integrity

Female MS patients in contrast to male MS patients had higher clustering coefficient ( $P = 0.012$ ) (Fig. 2). In both female and male MS patients, the molecular layer was identified as a hub.

When comparing the subfields between female and male MS patients, females showed lower volumes of parasubiculum, presubiculum and hippocampal fissure (all  $P < 0.001$ ) and greater volumes of the molecular layer ( $P < 0.001$ ) (Fig. 3, Table 3). There were no significant differences in the volumes of other subfields (all  $P > 0.05$ ). In HS counterparts, no sex-specific differences in the baseline volumes of either subfield were detectable (all  $P > 0.05$ ) but a trend with similar direction as in MS patients for molecular layer ( $P = 0.05$ ) and hippocampal fissure ( $P = 0.08$ ) (Fig. 3).



**Table 2. Summary of the linear mixed effects model for hippocampal network parameters.**

	MS patients				Healthy subjects				F	P
	Female		Male		Female		Male			
	B	FU	B	FU	B	FU	B	FU		
Clustering coefficient	0.132 (0.03)	0.136 (0.04)	0.131 (0.02)	0.134 (0.04)	0.117 (0.03)	0.120 (0.02)	0.117 (0.04)	0.123 (0.04)		
Group									20.11	P<0.001
Sex									12.10	P<0.001
Time									31.17	P<0.001
Sex × time									12.77	P<0.001

Variables are presented as adjusted means (standard deviation).  
Significant P-values (Bonferroni corrected for multiple comparisons) are marked in bold.  
B, baseline; FU, follow-up.

## Over time multiple sclerosis females develop an even more clustered network organization along with widespread regional tissue loss

Longitudinally, female MS patients exhibited an increase in clustering coefficient ( $P < 0.001$ ) (Fig. 2), with follow-up values higher than in male MS patients ( $P = 0.014$ ). At follow-up, the molecular layer remained the hub node in this patient group.

These network dynamics occurred along with extensive regional volume loss across most of the subfields—presubiculum, subiculum, CA1, CA3, CA4, granule cell layer of the dentate gyrus, hippocampus-amygdala transition area, molecular layer, hippocampal tail and whole hippocampus (all  $P < 0.001$ ) (Fig. 3). Contrary to this, over time HS females showed much less regional tissue loss compared to MS females, limited merely to parasubiculum and presubiculum (both  $P < 0.001$ ) and sparing other subfields (Fig. 3).

## Over time multiple sclerosis males develop an even more clustered network organization and less widespread regional tissue loss

Longitudinally, male MS patients presented an increase in clustering coefficient ( $P < 0.001$ ) (Fig. 2). At follow-up, the molecular layer remained the hub node as well in male MS patients.

Hippocampal integrity was characterized by progressive volume loss in fewer hippocampal subfields compared to female MS patients—presubiculum, subiculum, CA4, granule cell layer of the dentate gyrus, fimbria, molecular layer and whole hippocampus (all  $P < 0.01$ ) (Fig. 3). Compared to male MS patients, over time HS males manifested regional volume loss exclusively in parasubiculum and fimbria (both  $P < 0.001$ ), rest of the regions remaining intact (Fig. 3).

## Cognition is differentially related to hippocampal network architecture and structural integrity in multiple sclerosis females and males

The composite cognitive performance score was positively associated with clustering coefficient in female ( $B = 2.3$ , s.e.m. = 1.5,  $P = 0.013$ ) but not in male ( $B = 0.7$ , s.e.m. = 2.2,  $P = 0.74$ ) MS patients (Fig. 4). In female MS patients, the composite cognitive performance score was positively associated with the volumes of CA1 ( $B = 0.001$ , s.e.m. = 0.001,  $P = 0.020$ ), CA3 ( $B = 0.003$ , s.e.m. = 0.003,  $P = 0.010$ ), CA4 ( $B = 0.001$ , s.e.m. = 0.003,  $P = 0.013$ ), granule cell layer of dentate gyrus ( $B = 0.001$ , s.e.m. = 0.002,  $P = 0.022$ ), hippocampus-

**Table 3. Summary of the linear mixed effects models<sup>a</sup> for hippocampal subfield volumes.**

	MS patients				Healthy subjects				F	P
	Female		Male		Female		Male			
	B	FU	B	FU	B	FU	B	FU		
Parasubiculum Group	57.8 ± 9.4	57.5 ± 9.6	65.6 ± 10.3	65.3 ± 10.8	59.8 ± 9.0	57.8 ± 8.5	66.1 ± 10.3	62.9 ± 10.4	24.70	P<0.001
Sex									20.30	P<0.001
Time									39.30	P<0.001
Sex × time									2.07	P=0.090
Presubiculum Group	293.1 ± 32.5	288.1 ± 32.7	320.5 ± 38.1	315.4 ± 36.8	303.5 ± 30.4	295.4 ± 31.7	331.7 ± 40.2	321.3 ± 37.7	18.01	P<0.001
Sex									9.22	P<0.001
Time									35.85	P<0.001
Sex × time									0.88	P=0.466
Subiculum Group	427.7 ± 42.1	424.5 ± 43.0	461.9 ± 46.3	457.2 ± 44.3	431.8 ± 41.4	427.3 ± 38.7	467.1 ± 48.8	462.4 ± 48.0	1.35	P=0.216
Sex									0.45	P=0.117
Time									12.01	P<0.001
Sex × time									0.45	P=0.524
CA1 Group	619.2 ± 68.0	613.8 ± 64.1	683.7 ± 67.9	679.1 ± 67.8	638.3 ± 24.6	629.0 ± 23.6	687.1 ± 69.1	679.5 ± 69.3	12.11	P<0.001
Sex									0.09	P=0.781
Time									15.02	P<0.001
Sex × time									8.33	P<0.001
CA3 Group	200.2 ± 26.9	201.0 ± 27.2	219.0 ± 27.7	220.6 ± 25.6	213.4 ± 23.7	210.8 ± 22.1	231.1 ± 25.0	228.5 ± 23.6	28.30	P<0.001
Sex									0.33	P=0.322
Time									9.15	P<0.001
Sex × time									1.70	P=0.209
CA4 Group	248.6 ± 26.5	248.7 ± 26.1	273.3 ± 29.0	274.6 ± 27.0	261.0 ± 24.9	256.4 ± 24.4	280.3 ± 29.9	275.3 ± 28.7	47.02	P<0.001
Sex									1.01	P=0.239
Time									23.11	P<0.001
Sex × time									1.87	P=0.158
GCDG Group	291.2 ± 30.3	290.9 ± 30.6	322.31 ± 33.0	320.3 ± 33.4	302.3 ± 28.9	297.3 ± 28.1	323.4 ± 35.6	323.0 ± 33.9	33.46	P<0.001
Sex									0.31	P=0.602
Time									17.90	P<0.001
Sex × time									0.86	P=0.115
HATA Group	59.5 ± 8.4	59.3 ± 8.3	65.6 ± 8.5	64.5 ± 8.6	62.6 ± 6.7	61.5 ± 6.3	68.0 ± 7.7	67.3 ± 7.5	51.77	P<0.001
Sex									0.88	P=0.370
Time									9.33	P<0.001
Sex × time									1.92	P=0.203
Fimbria	80.3 ± 17.1	78.8 ± 16.8	86.3 ± 18.7	82.2 ± 18.8	86.4 ± 15.5	83.7 ± 16.1	99.5 ± 14.1	94.9 ± 14.3		

(continued)

Table 3. Continued

	MS patients				Healthy subjects				F	P
	Female		Male		Female		Male			
	B	FU	B	FU	B	FU	B	FU		
Group									19.60	P < 0.001
Sex									0.77	P = 0.590
Time									11.51	P < 0.001
Sex × time									1.22	P = 0.104
Molecular layer	610.6 ± 57.9	606.0 ± 59.9	558.8 ± 54.1	554.6 ± 52.2	614.0 ± 61.1	612.4 ± 63.1	571.8 ± 48.7	562.4 ± 48.9		
Group									20.92	P < 0.001
Sex									35.38	P < 0.001
Time									27.14	P < 0.001
Sex × time									12.03	P < 0.001
Hippocampal fissure	147.0 ± 21.7	144.2 ± 23.1	166.7 ± 23.1	164.5 ± 21.2	142.1 ± 57.2	144.1 ± 59.1	155.6 ± 23.3	155.0 ± 20.5		
Group									14.03	P < 0.001
Sex									9.51	P < 0.001
Time									0.66	P = 0.302
Sex × time									5.57	P = 0.011
Hippocampal tail	506.9 ± 67.2	495.1 ± 65.5	539.6 ± 69.4	533.3 ± 70.7	541.0 ± 66.4	534.5 ± 65.2	586.6 ± 58.3	577.5 ± 58.5		
Group									29.10	P < 0.001
Sex									0.11	P = 0.663
Time									10.08	P < 0.001
Sex × time									7.22	P = 0.008
Whole hippocampus	3396.3 ± 309.7	3363.6 ± 296.8	3679.4 ± 336.7	3641.7 ± 335.7	3425.8 ± 284.5	3384.7 ± 275.7	3751.5 ± 355.1	3702.6 ± 338.9		
Group									1.01	P = 0.199
Sex									41.80	P < 0.001
Time									50.79	P < 0.001
Sex × time									1.18	P = 0.261

Variables are presented as adjusted means  $\pm$  standard deviation.

<sup>a</sup>Linear models were adjusted for total intracranial volume, age and centre.

Significant  $P$ -values (Bonferroni corrected for multiple comparisons) are marked in bold.

B, baseline; CA1, 3, 4, cornu ammonis 1, 3, 4; FU, follow-up; GCDG, granule cell layer of dentate gyrus; HATA, hippocampus-amygdala transition area.

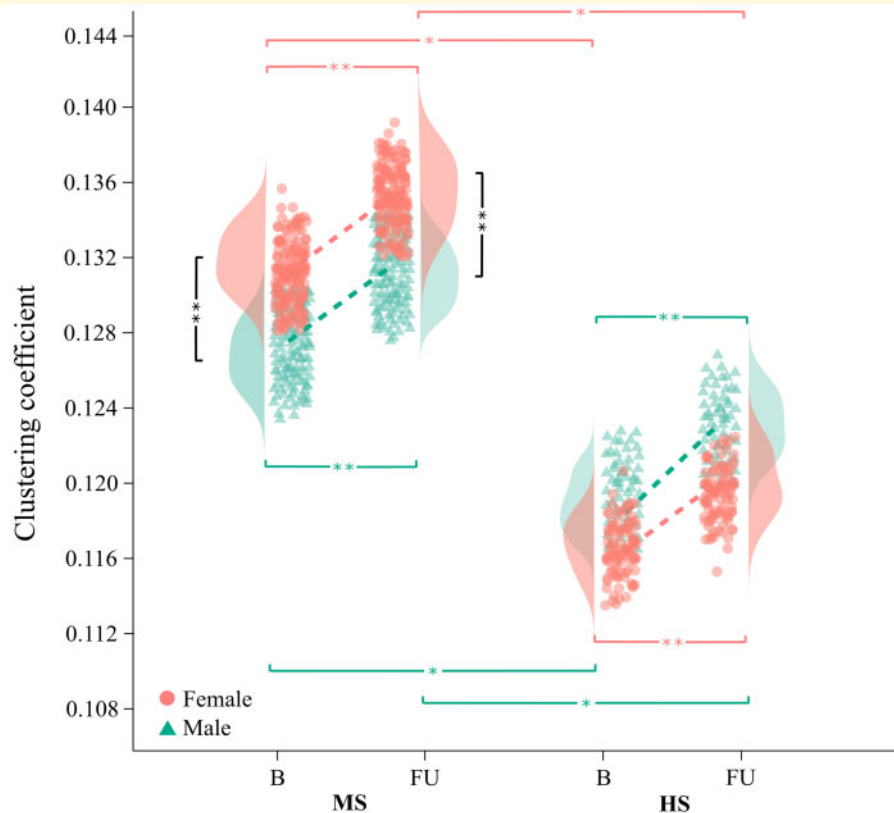


**Figure 2 Sex-specific differences in hippocampal network organization.** Results from the linear mixed effects model showing sex differences in network measures (clustering coefficient) in multiple sclerosis (MS) patients and healthy subjects (HS) at baseline (B) and follow-up (FU); \* $P < 0.01$ , \*\* $P < 0.001$  (Bonferroni corrected for multiple comparisons).

amygdala transition area ( $B = 0.008$ , s.e.m. = 0.009,  $P = 0.001$ ) and molecular layer ( $B = 0.001$ , s.e.m. = 0.001,  $P = 0.019$ ) (Fig. 5). In males, the composite cognitive performance score was related to the volumes of CA1 ( $B = 0.001$ , s.e.m. = 0.002,  $P = 0.019$ ) and molecular layer ( $B = 0.001$ , s.e.m. = 0.002,  $P = 0.022$ ) (Fig. 5).

The composite memory performance score was positively associated with clustering coefficient in female ( $B = 1.9$ , s.e.m. = 1.4,  $P = 0.001$ ) but not in male ( $B = 0.8$ , s.e.m. = 1.2,  $P = 0.24$ ) MS patients (Fig. 4). In female MS patients, the composite memory performance score was associated with the volumes of presubiculum ( $B = -0.004$ , s.e.m. = 0.002,  $P = 0.046$ ), CA3 ( $B = 0.007$ , s.e.m. = 0.002,  $P = 0.001$ ), CA4 ( $B = 0.005$ , s.e.m. = 0.002,  $P = 0.011$ ), granule cell layer of dentate gyrus ( $B = 0.004$ , s.e.m. = 0.002,  $P = 0.027$ ) and fimbria ( $B = -0.007$ , s.e.m. = 0.003,  $P = 0.012$ ) (Fig. 5). In males, the composite memory performance score was related only to the volume of hippocampus-amygdala transition area ( $B = 0.01$ , s.e.m. = 0.007,  $P = 0.048$ ) (Fig. 5).

Additionally, a trend for a positive association between EDSS and clustering coefficient ( $B = 0.003$ , s.e.m. = 0.002,  $P = 0.06$ , Fig. 4) was observed only in female MS patients. Longer disease duration was positively

associated with a higher clustering coefficient in females ( $B = 0.0002$ , s.e.m. = 0.0001,  $P = 0.008$ ) but not in males ( $B = 0.00004$ , s.e.m. = 0.0007,  $P = 0.69$ , Fig. 4) MS patients. Sex-specific negative associations between EDSS, disease duration and volumes of hippocampal subfields are presented in Supplementary Material.

Hippocampal lesion volumes were not related to any of the network parameters (all  $P > 0.05$ ) neither in female nor in male MS patients, perhaps, suggesting a higher sensitivity of hippocampal networks to neurodegeneration, rather than to inflammatory injury.

## Discussion

By modelling single-subject intrinsic networks and quantifying subfield volumetric variations, we were able to detect sex-specific differences in hippocampal vulnerability in MS patients. In particular, we show that in both female and male MS patients the hippocampal network topology is more clustered compared to HS, although, more prominent in female patients. As time elapses, a similar pattern of network reorganization towards an even more clustered, and predominantly in female



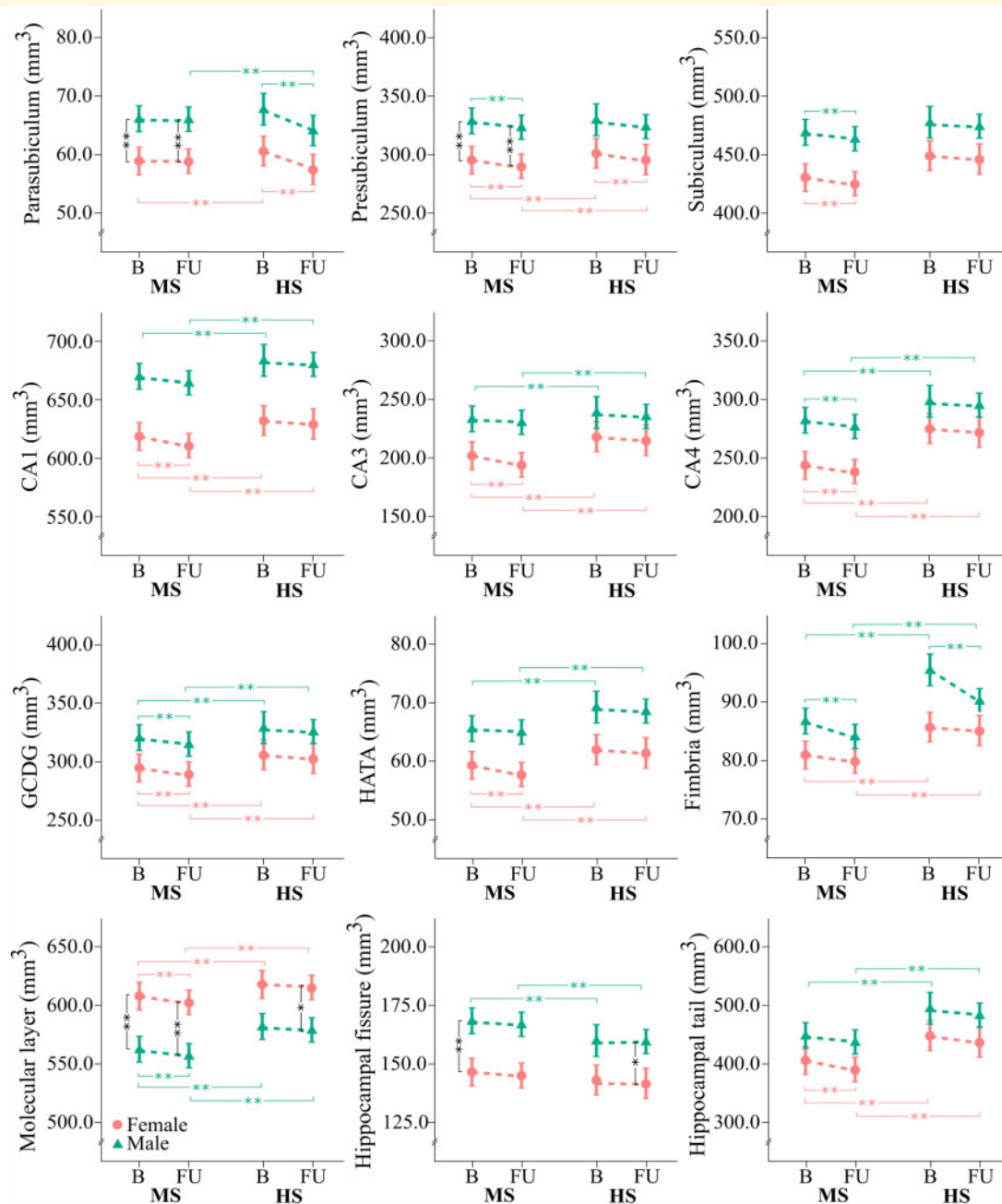
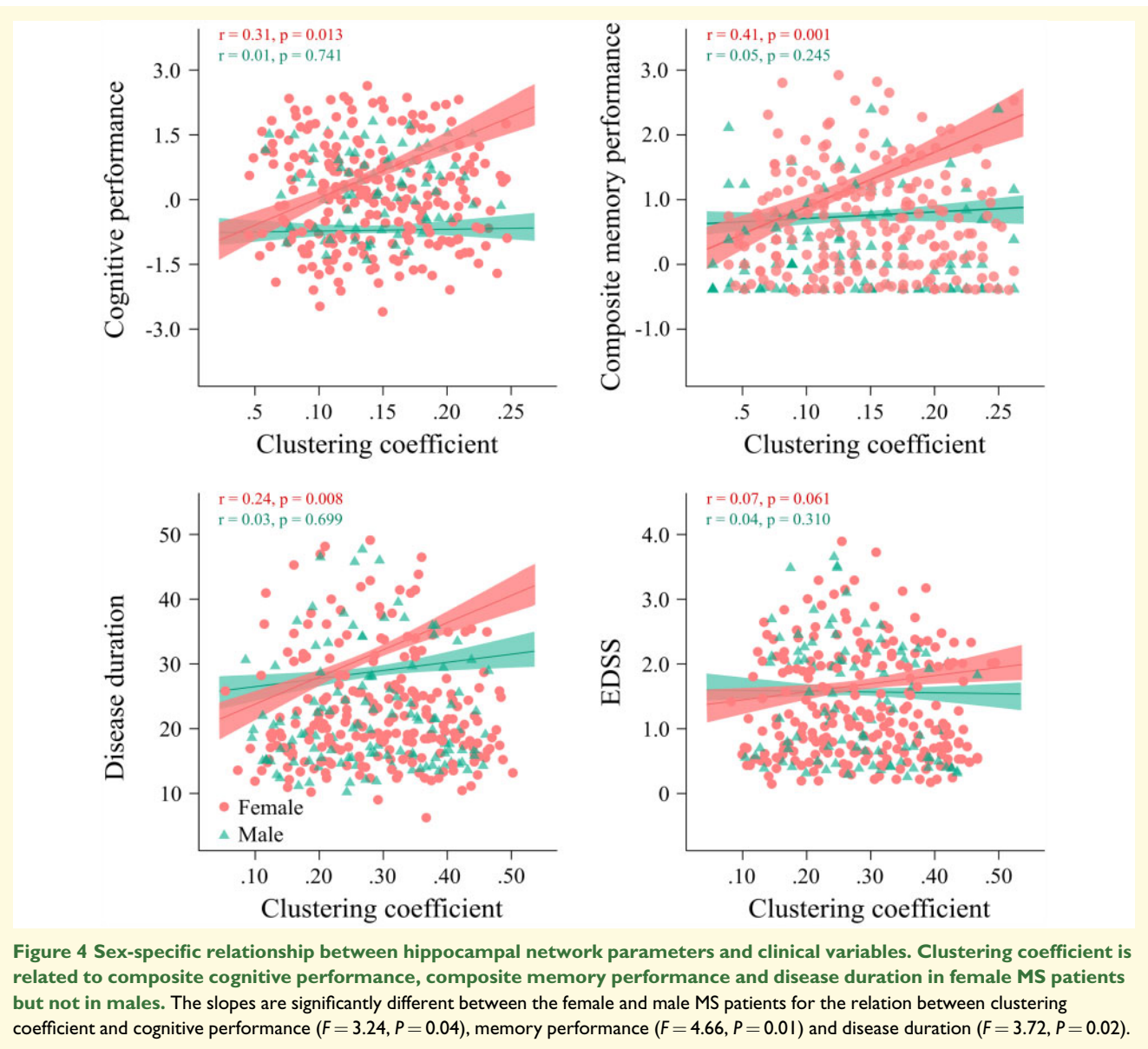


**Figure 3 Sex-specific differences in hippocampal subfield volumes.** Results from the linear mixed effects models showing sex differences in the volumes of hippocampal subfields in multiple sclerosis (MS) patients and healthy subjects (HS) at baseline (B) and follow-up (FU). Error bars with 95% confidence intervals are presented; \* $P < 0.01$ , \*\* $P < 0.001$  (Bonferroni corrected for multiple comparisons). CA1, 3, 4 = cornu ammonis 1, 3, 4; GCDG, granule cell layer of dentate gyrus; HATA, hippocampus-amygdala transition area.

patients is retained. These network alterations occurred along with regional structural alterations. Specifically, male and female MS patients presented widespread regional subfield atrophy compared to HS, however, with a more extensive involvement observed in female patients over time. The described hippocampal network and anatomical organization were related to cognitive performance more tightly in females than in male MS patients.

### Sex-specific signatures of hippocampal morphometric networks

Identifying the sex-specific phenotypes of hippocampal networks is a step forward in characterizing the network reorganization at the interplay of MS pathology and sex. The obtained measures of hippocampal network topology imply concomitantly occurring processes—increased local



structural similarity and long-range structural dissimilarity, possibly related to disconnection mechanisms.<sup>12</sup> Hippocampal tissue remodelling elicited by MS destructive and restorative processes might underlie the observed vector in the network behaviour.<sup>38–40</sup> This pattern of a more clustered network organization is maintained over time regardless of sex, perhaps, as an adaptive response to ongoing localized inflammation and degeneration. This speculation is supported by the observations of more atrophied subfields with time in female patients, which have a more clustered network configuration than the male patients. As it has been recently shown by our group, the increased local connectivity is possibly a compensation mechanism to structural damage aimed to reinforce the brain network functionality.<sup>13,33,38,41</sup> These

principles of network reorganization to MS injury might be extrapolated to hippocampal networks.

Studies on sex differences in hippocampal networks in patients with MS are lacking so far. Available studies investigating whole-brain functional networks have not been able to identify any between-sex differences in MS patients.<sup>42</sup> Our results indicate that female MS patients display a more clustered network architecture than male patients both at baseline and after 2 years of follow-up. Several explanations for this exist. First, a more amplified compensation response of local network connectivity to a more compromised regional integrity in female patients might be hypothesized. Second, higher hippocampal connectivity in female patients might emerge from overall higher brain connectivity in females than in males as

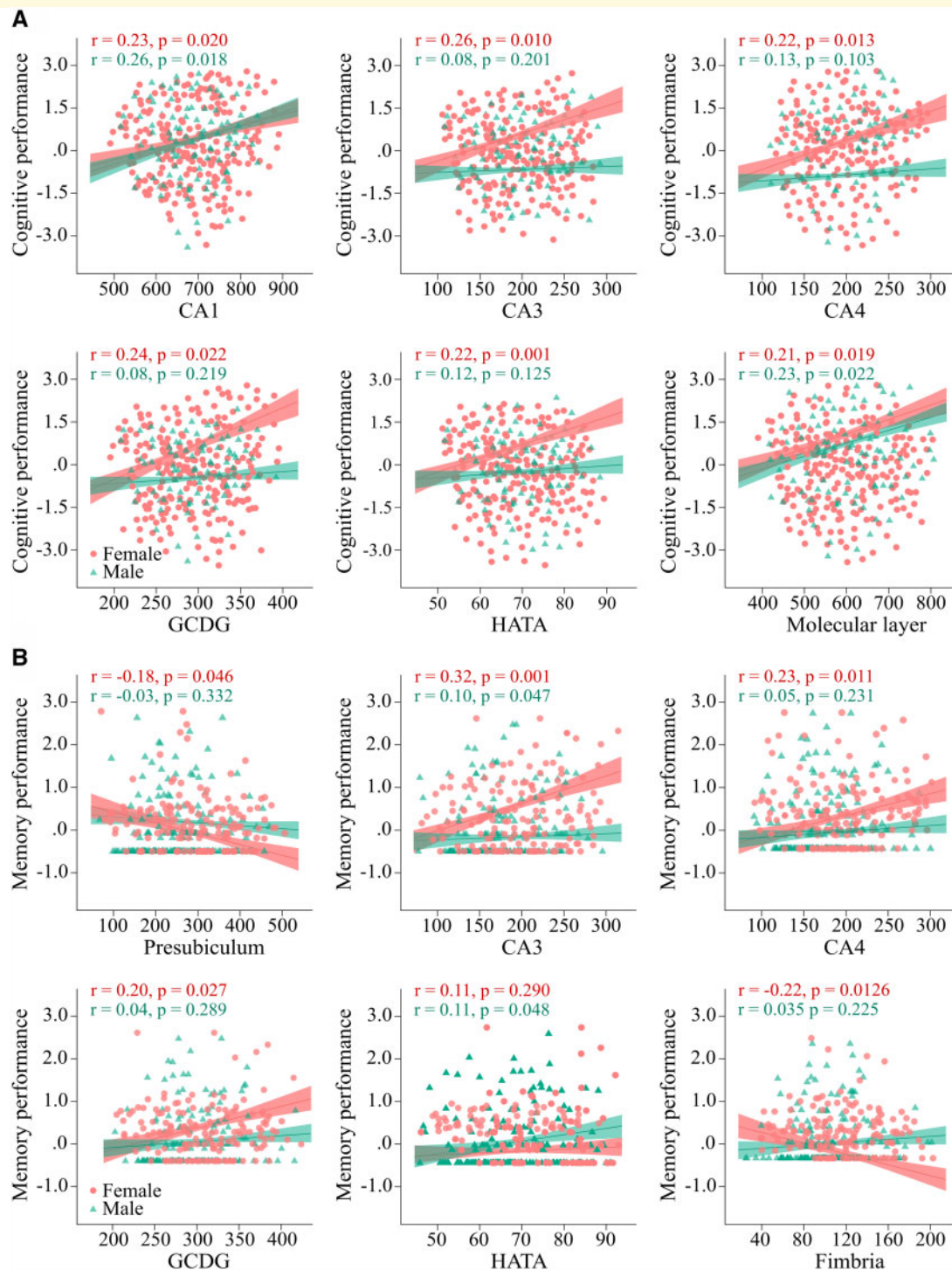


**Figure 5 Sex-specific relationship between hippocampal subfield volumes and cognitive and memory performance. (A)** Significant associations between composite cognitive performance and subfield volumes in female (cornu ammonis 1/3/4—CA1/CA3/CA4, granule cell layer of dentate gyrus—GCDG, hippocampus-amygdala transition area—HATA, molecular layer) and male (CA1, molecular layer) MS patients. The slopes are significantly different between the female and male MS patients for the relation between cognitive performance and volumes of CA3 ( $F = 3.44, P = 0.03$ ), CA4 ( $F = 3.20, P = 0.04$ ), CCDG ( $F = 3.42, P = 0.03$ ) and HATA ( $F = 3.55, P = 0.02$ ). **(B)** Significant associations between composite memory performance and subfield volumes in female (presubiculum, cornu ammonis 3/4—CA3/CA4, granule cell layer of dentate gyrus—GCDG, fimbria) and male (hippocampus-amygdala transition area—HATA) MS patients. The slopes are significantly different between the female and male MS patients for the relation between memory performance and volumes of presubiculum ( $F = 3.64, P = 0.03$ ), CA3 ( $F = 4.31, P = 0.02$ ), CA4 ( $F = 4.99, P = 0.01$ ), CCDG ( $F = 3.91, P = 0.02$ ) and fimbria ( $F = 4.03, P = 0.02$ ).



shown in this (Supplementary Material), as well as in other works.<sup>43,44</sup> Third, as sex steroids exert different effects on certain cortical or/and subcortical regions as parts of structural and functional networks in females and males,<sup>45</sup> distinct effects of sex steroids on hippocampal network architecture and functionality might be expected.<sup>46,47</sup> Hence, hippocampal network reorganization is an integrated, yet the sex-modulated response to physiological and pathological processes.

## Sex-specific signatures of hippocampal anatomic compartments

Involvement of the hippocampal tissue integrity, occurring early during the disease course of MS, translates into reduced whole and regional hippocampal volumes.<sup>48–50</sup> Previous studies exploring sex effects on hippocampal volumes did not find any differences in the whole hippocampal volume between female and male MS patients.<sup>3,51</sup> We show that both female and male MS patients have lower volumes in almost all hippocampal subfields compared to healthy females and males. Several pathophysiological processes, ranging from inflammatory demyelination, decreased dendritic and axonal density to neuronal cell loss and gliosis have been proposed as primers of regional hippocampal atrophy in MS.<sup>52,53</sup> One must be confident that additionally to sex, variation in the volumes of distinct hippocampal subfields might be attributed to different factors that selectively impact the integrity of the subfields, i.e. age,<sup>54,55</sup> brain volume changes during the life span,<sup>56</sup> cardiovascular, pro-inflammatory and APOE $\epsilon$ 4 risk factors.<sup>57</sup>

Sex-specific differences in regional hippocampal microstructural and physiological properties in response to acute and chronic MS neuroinflammatory damage have not been previously characterized in MS patients. In this respect, several observations might support our findings: (i) animal models of MS show sex differences in immune cell and cytokine repertoire and disease severity,<sup>46</sup> (ii) regional hippocampal integrity relates to cerebrospinal fluid (CSF) inflammatory markers impacting synaptic plasticity and cognitive function in MS patients,<sup>58</sup> and (iii) high GM atrophy rates in MS patients are associated with high CSF levels of immunoglobulins.<sup>59</sup> By comparing female and male MS patients, we show that regional volumetric differences are evident in particular subfields, with lower volumes of pre- and parasubiculum but higher volumes of the molecular layer in female patients. However, over time the neurodegenerative process entrains the majority of hippocampal subfields with more regions affected in female patients. The reasons for these results remain unclear but a sex-specific imbalance between neural damage and repair processes is driven by a multifactorial interaction between immune cells,

inflammatory mediators and sex steroids on one side and neuronal cell, axonal and myelin turnover on the other side, is very likely.<sup>46</sup>

## Hippocampal network and anatomical correlates of cognitive performance

Existing evidence strongly suggests that females and males differentially recruit hippocampal networks during cognitive tasks.<sup>60</sup> Previous studies claimed that male MS patients perform worse than female patients in several cognitive domains, including processing speed, verbal memory and executive functioning.<sup>3,61</sup> However, in our cohort, cognitive and memory performance scores did not differ between female and male patients, perhaps, due to the early disease stage or the sensitivity of applied screening tests.<sup>62</sup> Positive associations between higher clustering and better cognitive and memory performance scores only in female MS patients suggests that females might integrate more efficiently the hippocampal networks into the global brain networks<sup>63</sup> mediating the information processing and superior verbal memory in females compared to males,<sup>64,65</sup> respectively. Alternatively, females might activate more limbic networks, including the hippocampal and prefrontal networks, whereas males recruit more distributed networks during cognitive tasks relying on working memory performance.<sup>66</sup>

The here depicted associations between hippocampal subfield integrity and cognitive and memory performance scores support previous findings showing that along with cortical and subcortical GM structures<sup>67</sup> the hippocampus is also involved in information processing speed, cognitive flexibility and reserve.<sup>64,68,69</sup> We extend these data and show that cognitive and memory performance scores are related to the volumes of more subfields in female MS patients than in male patients. These findings endorse the obtained correlations between the network topology and cognitive and memory performance scores in female MS patients, suggesting that females rely more on hippocampal networks than males during the execution of cognitive tasks involving processing speed and verbal memory. Most of the previous studies in MS reported mainly the relation between cognitive and memory impairment and the integrity of the CA1 region.<sup>48–50</sup> Thus, our work represents a step forward into a more detailed characterization of the correlates of cognitive and memory performance in MS.

## Strengths, limitations and perspectives

The following strengths of the current study are worth to be mentioned. First, the inclusion of a large cohort of MS patients with closely matched healthy controls. Second, the



longitudinal design of the study allowed us to investigate the time effects on the variables. Third, by modelling the subject-specific morphometric networks, individual trends of network dynamics have been captured. Several limitations apply to this study. The relatively short follow-up period of two years, which was, however, enough to capture the sex-specific trajectories of hippocampal network reorganization and regional atrophy. The employed here neuropsychological tests are screening tools and might be less sensitive in detecting sex-specific variations in cognitive impairment at early disease stages of MS.<sup>62</sup> One can assume that the obtained results could be biased by including more female than male MS patients. Nevertheless, this bias was mitigated by applying mixed-effects models and comparing MS patients to their healthy sex counterparts. Considering the potential effects of the type of scanner and acquisition parameters on the accuracy of hippocampal segmentation, we included the type of scanner as a confounding factor. In addition, hippocampal segmentation performed in FreeSurfer shows high reliability across different scanner platforms.<sup>28</sup> Given the interethnic differences in brain morphometry,<sup>70,71</sup> inclusion in our study of HS of different ethnicities might have influenced our observations. This and other aspects of sex-specific differences in the hippocampal organization might be addressed in target works. As the spatial location of lesions predetermines the patterns of GM pathology,<sup>72</sup> identification of sex-specific responses of hippocampal networks and regional integrity to the spatial distribution of intrahippocampal lesions might be of interest.

## Conclusions

Our observations suggest a more clustered pattern of hippocampal network organization in females than in male MS patients that are preserved with the disease evolution. Sex-specific network reorganization follows the structural pattern of more extensive atrophy of hippocampal compartments in female MS patients over time. The differential relation of cognitive performance to hippocampal network and regional substrates might explain the variability in cognitive functioning and advance the development of personalized sex-targeted cognitive rehabilitation strategies, aimed to combat the accrual of cognitive burden.

## Supplementary material

Supplementary material is available at *Brain Communications* online.

## Acknowledgements

We are grateful for the computing time granted on Magon supercomputer for processing of neuroimaging data and for advisory services offered by Johannes Gutenberg University

Mainz (hpc.uni-mainz.de), which is a member of the AHRP and the Gauss Alliance e. V. Also, we would like to thank SLIM and OASIS repositories for data availability.

## Funding

This study was supported by the German Research Foundation (DFG; CRC-TR-128).

## Competing interests

The authors report no competing interests.

## References

1. Voskuhl RR, Gold SM. Sex-related factors in multiple sclerosis susceptibility and progression. *Nat Rev Neurol*. 2012;8(5):255–263.
2. Antulov R, Weinstock-Guttman B, Cox J, et al. Gender-related differences in MS: A study of conventional and nonconventional MRI measures. *Mult Scler J*. 2009;15(3):345–354.
3. Schoonheim MM, Popescu V, Lopes FCR, et al. Subcortical atrophy and cognition: Sex effects in multiple sclerosis. *Neurology*. 2012;79(17):1754–1761.
4. Lin S-J, Lam J, Beveridge S, et al. Cognitive performance in subjects with multiple sclerosis is robustly influenced by gender in canonical-correlation analysis. *J Neuropsychiatry Clin Neurosci*. 2017;29(2):119–127.
5. Beatty WW, Aupperle RL. Sex differences in cognitive impairment in multiple sclerosis. *Clin Neuropsychol*. 2002;16(4):472–480.
6. Mégevand P, Groppe DM, Bickel S, et al. The hippocampus and amygdala are integrators of neocortical influence: A corticocortical evoked potential study. *Brain Connect*. 2017;7(10):648–660.
7. Maller JJ, Welton T, Middione M, Callaghan FM, Rosenfeld JV, Grieve SM. Revealing the hippocampal connectome through super-resolution 1150-direction diffusion MRI. *Sci Rep*. 2019;9(1):2418–2413.
8. Knierim JJ. The hippocampus. *Curr Biol*. 2015;25(23):R1116–R1121.
9. Rocca MA, Barkhof F, De Luca J, et al. The hippocampus in multiple sclerosis. *Lancet Neurol*. 2018;17(10):918–926.
10. Morelli ME, Baldini S, Sartori A, et al. Early putamen hypertrophy and ongoing hippocampus atrophy predict cognitive performance in the first ten years of relapsing-remitting multiple sclerosis. *Neuro Sci*. 2020;41(10):2893–2904.
11. González Torre JA, Cruz-Gómez ÁJ, Belenguer A, Sanchis-Segura C, Ávila C, Forn C. Hippocampal dysfunction is associated with memory impairment in multiple sclerosis: A volumetric and functional connectivity study. *Mult Scler J*. 2017;23(14):1854–1863.
12. Fleischer V, Radetz A, Ciolac D, et al. Graph theoretical framework of brain networks in multiple sclerosis: A review of concepts. *Neuroscience*. 2019;403:35–53. doi: 10.1016/j.neuroscience.2017.10.033
13. Fleischer V, Koirala N, Drobny A, et al. Longitudinal cortical network reorganization in early relapsing-remitting multiple sclerosis. *Ther Adv Neurol Disord*. 2019;12:1756286419838673.
14. Charalambous T, Tur C, Prados F, et al. Structural network disruption markers explain disability in multiple sclerosis. *J Neurol Neurosurg Psychiatry*. 2019;90(2):219–226.
15. Ciolac D, Luessi F, Gonzalez-Escamilla G, et al. Selective brain network and cellular responses upon dimethyl fumarate immunomodulation in multiple sclerosis. *Front Immunol*. 2019;10:1779.

16. Polman CH, Reingold SC, Banwell B, et al. Diagnostic criteria for multiple sclerosis: 2010 revisions to the McDonald criteria. *Ann Neurol*. 2011;69(2):292–302.
17. Rao S. A manual for the Brief Repeatable Battery of neuropsychological tests in multiple sclerosis. New York, NY: National Multiple Sclerosis Society; 1990.
18. Cutter GR, Baier ML, Rudick RA, et al. Development of a multiple sclerosis functional composite as a clinical trial outcome measure. *Brain*. 1999;122(5):871–882.
19. Calabrese P, Kalbe E, Kessler J. Ein neuropsychologisches Screening zur Erfassung kognitiver Störungen bei MS-Patienten-Das Multiple Sklerose Inventarium Cognition (MUSIC). *Psychoneuro*. 2004;30(7):384–388.
20. Scherer P, Baum K, Bauer H, Göhler H, Miltenburger C. Normierung der brief repeatable battery of neuropsychological tests (BRB-N) für den deutschsprachigen Raum. *Der Nervenarzt*. 2004;75(10):984–990.
21. Liu W, Wei D, Chen Q, et al. Longitudinal test-retest neuroimaging data from healthy young adults in southwest China. *Sci Data*. 2017;4:170017.
22. LaMontagne PJ, Benzinger TLS, Morris JC, et al. OASIS-3: Longitudinal neuroimaging, clinical, and cognitive dataset for normal aging and Alzheimer disease. *medRxiv*. 2019. doi: 10.1101/2019.12.13.19014902.
23. Fischl B. FreeSurfer. *Neuroimage*. 2012;62(2):774–781.
24. Reuter M, Schmansky NJ, Rosas HD, Fischl B. Within-subject template estimation for unbiased longitudinal image analysis. *Neuroimage*. 2012;61(4):1402–1418.
25. Desikan RS, Ségonne F, Fischl B, et al. An automated labeling system for subdividing the human cerebral cortex on MRI scans into gyral based regions of interest. *Neuroimage*. 2006;31(3):968–980.
26. Iglesias JE, Augustinack JC, Nguyen K, et al. A computational atlas of the hippocampal formation using ex vivo, ultra-high resolution MRI: Application to adaptive segmentation of in vivo MRI. *Neuroimage*. 2015;115:117–137.
27. Whelan CD, Hibar DP, van Velzen LS, et al. Heritability and reliability of automatically segmented human hippocampal formation subregions. *Neuroimage*. 2016;128:125–137.
28. Brown EM, Pierce ME, Clark DC, et al. Test-retest reliability of FreeSurfer automated hippocampal subfield segmentation within and across scanners. *Neuroimage*. 2020;210:116563.
29. Pintzka CWS, Hansen TI, Evensmoen HR, Håberg AK. Marked effects of intracranial volume correction methods on sex differences in neuroanatomical structures: A HUNT MRI study. *Front Neurosci*. 2015;9:238.
30. Nordenskjöld R, Malmberg F, Larsson E-M, et al. Intracranial volume normalization methods: Considerations when investigating gender differences in regional brain volume. *Psychiatry Res Neuroimaging*. 2015;231(3):227–235.
31. Nebli A, Reikik I. Gender differences in cortical morphological networks. *Brain Imaging Behav*. 2020;14(5):1831–1839.
32. Rubinov M, Sporns O. Complex network measures of brain connectivity: Uses and interpretations. *Neuroimage*. 2010;52(3):1059–1069. doi:10.1016/j.neuroimage.2009.10.003
33. Muthuraman M, Fleischer V, Kolber P, Luessi F, Zipp F, Groppa S. Structural brain network characteristics can differentiate CIS from early RRMS. *Front Neurosci*. 2016;10:14.
34. Ciolac D. Remodeling of cortical structural networks in multiple sclerosis. New York, NY: Springer; 2019:491–495.
35. Onnela J-P, Saramäki J, Kertész J, Kaski K. Intensity and coherence of motifs in weighted complex networks. *Phys Rev E*. 2005; 71(6):065103.
36. van den Heuvel MP, Sporns O. Network hubs in the human brain. *Trends Cogn Sci*. 2013;17(12):683–696.
37. Schmidt P, Gaser C, Arsic M, et al. An automated tool for detection of FLAIR-hyperintense white-matter lesions in Multiple Sclerosis. *Neuroimage*. 2012;59(4):3774–3783. doi: 10.1016/j.neuroimage.2011.11.032
38. Fleischer V, Groger A, Koirala N, et al. Increased structural white and grey matter network connectivity compensates for functional decline in early multiple sclerosis. *Mult Scler*. 2017;23(3): 432–441. doi:10.1177/1352458516651503
39. Cerina M, Muthuraman M, Gallus M, et al. Myelination-and immune-mediated MR-based brain network correlates. *J Neuroinflamm*. 2020;17(1):186–116.
40. Zhou F, Zhuang Y, Wang L, et al. Disconnection of the hippocampus and amygdala associated with lesion load in relapsing–remitting multiple sclerosis: A structural and functional connectivity study. *Neuropsychiatry Dis Treat*. 2015;11:1749.
41. Gonzalez-Escamilla G, Ciolac D, De Santis S, et al. Gray matter network reorganization in multiple sclerosis from 7-Tesla and 3-Tesla MRI data. *Ann Clin Transl Neurol*. 2020;7(4):543–553.
42. Schoonheim MM, Hulst HE, Landi D, et al. Gender-related differences in functional connectivity in multiple sclerosis. *Mult Scler J*. 2012;18(2):164–173.
43. Gong G, Rosa-Neto P, Carbonell F, Chen ZJ, He Y, Evans AC. Age- and gender-related differences in the cortical anatomical network. *J Neurosci*. 2009;29(50):15684–15693.
44. Gong G, He Y, Evans AC. Brain connectivity: Gender makes a difference. *Neuroscientist*. 2011;17(5):575–591.
45. Peper JS, van den Heuvel MP, Mandl RC, Pol HEH, van Honk J. Sex steroids and connectivity in the human brain: A review of neuroimaging studies. *Psychoneuroendocrinology*. 2011;36(8): 1101–1113.
46. Ysraelit MC, Correale J. Impact of sex hormones on immune function and multiple sclerosis development. *Immunology*. 2019; 156(1):9–22.
47. Avila M, Bansal A, Culbertson J, Peiris AN. The role of sex hormones in multiple sclerosis. *Eur Neurol*. 2018;80(1-2):93–99.
48. Planche V, Koubiyr I, Romero JE, et al. Regional hippocampal vulnerability in early multiple sclerosis: Dynamic pathological spreading from dentate gyrus to CA 1. *Hum Brain Mapp*. 2018; 39(4):1814–1824.
49. Sicotte N, Kern K, Giesser B, et al. Regional hippocampal atrophy in multiple sclerosis. *Brain*. 2008;131(4):1134–1141.
50. Longoni G, Rocca MA, Pagani E, et al. Deficits in memory and visuospatial learning correlate with regional hippocampal atrophy in MS. *Brain Struct Funct*. 2015;220(1):435–444.
51. Dolezal O, Gabelic T, Horakova D, et al. Development of gray matter atrophy in relapsing–remitting multiple sclerosis is not gender dependent: Results of a 5-year follow-up study. *Clin Neurol Neurosurg*. 2013;115:S42–S48.
52. Geurts JJ, Bö L, Roosendaal SD, et al. Extensive hippocampal demyelination in multiple sclerosis. *J Neuropathol Exper Neurol*. 2007;66(9):819–827.
53. Papadopoulos D, Dukes S, Patel R, Nicholas R, Vora A, Reynolds R. Substantial archaocortical atrophy and neuronal loss in multiple sclerosis. *Brain Pathol*. 2009;19(2):238–253.
54. Pereira JB, Valls-Pedret C, Ros E, et al. Regional vulnerability of hippocampal subfields to aging measured by structural and diffusion MRI. *Hippocampus*. 2014;24(4):403–414.
55. Daugherty AM, Bender AR, Raz N, Ofen N. Age differences in hippocampal subfield volumes from childhood to late adulthood. *Hippocampus*. 2016;26(2):220–228.
56. Jakimovski D, Zivadinov R, Bergsland N, et al. Sex-specific differences in life span brain volumes in multiple sclerosis. *J Neuroimaging*. 2020;30(3):342–350.
57. Raz N, Daugherty AM, Bender AR, Dahle CL, Land S. Volume of the hippocampal subfields in healthy adults: Differential associations with age and a pro-inflammatory genetic variant. *Brain Struct Funct*. 2015;220(5):2663–2674.
58. Michailidou I, Willems JG, Kooi EJ, et al. Complement C 1q-C 3-associated synaptic changes in multiple sclerosis hippocampus. *Ann Neurol*. 2015;77(6):1007–1026.
59. Kroth J, Ciolac D, Fleischer V, et al. Increased cerebrospinal fluid albumin and immunoglobulin A fractions forecast cortical atrophy

- and longitudinal functional deterioration in relapsing-remitting multiple sclerosis. *Mult Scler.* 2019;25(3):338–343. doi: 10.1177/1352458517748474
60. Yagi S, Galea LA. Sex differences in hippocampal cognition and neurogenesis. *Neuropsychopharmacology.* 2019;44(1): 200–213.
  61. Savettieri G, Messina D, Andreoli V, et al. Gender-related effect of clinical and genetic variables on the cognitive impairment in multiple sclerosis. *J Neurol.* 2004;251(10):1208–1214.
  62. Johnen A, Bürkner P-C, Landmeyer NC, et al. Can we predict cognitive decline after initial diagnosis of multiple sclerosis? Results from the German National early MS cohort (KKNMS). *J Neurol.* 2019;266(2):386–312.
  63. Ingalhalikar M, Smith A, Parker D, et al. Sex differences in the structural connectome of the human brain. *Proc Natl Acad Sci USA.* 2014;111(2):823–828.
  64. Sundermann EE, Maki PM, Rubin LH, et al. Female advantage in verbal memory: Evidence of sex-specific cognitive reserve. *Neurology.* 2016;87(18):1916–1924.
  65. Asperholm M, Nagar S, Dekhtyar S, Herlitz A. The magnitude of sex differences in verbal episodic memory increases with social progress: Data from 54 countries across 40 years. *PLoS One.* 2019;14(4):e0214945.
  66. Hill AC, Laird AR, Robinson JL. Gender differences in working memory networks: A BrainMap meta-analysis. *Biol Psychol.* 2014; 102:18–29.
  67. Batista S, Zivadinov R, Hoogs M, et al. Basal ganglia, thalamus and neocortical atrophy predicting slowed cognitive processing in multiple sclerosis. *J Neurol.* 2012;259(1):139–146.
  68. Vuoksima E, Panizzon MS, Chen C-H, et al. Cognitive reserve moderates the association between hippocampal volume and episodic memory in middle age. *Neuropsychologia.* 2013;51(6):1124–1131.
  69. Perosa V, Priester A, Ziegler G, et al. Hippocampal vascular reserve associated with cognitive performance and hippocampal volume. *Brain.* 2020;143(2):622–634.
  70. Isamah N, Faison W, Payne ME, et al. Variability in frontotemporal brain structure: The importance of recruitment of African Americans in neuroscience research. *PLoS One.* 2010;5(10):e13642.
  71. Tang Y, Hojatkashani C, Dinov ID, et al. The construction of a Chinese MRI brain atlas: A morphometric comparison study between Chinese and Caucasian cohorts. *Neuroimage.* 2010;51(1): 33–41.
  72. Muthuraman M, Fleischer V, Kroth J, et al. Covarying patterns of white matter lesions and cortical atrophy predict progression in early MS. *Neurol Neuroimmunol Neuroinflamm.* 2020;7(3): e681.